

Control of force impulse in human-machine impact

*Original*

Control of force impulse in human-machine impact / DE BENEDICTIS, Carlo; Franco, Walter; Maffiodo, Daniela; Ferraresi, Carlo. - ELETTRONICO. - 49:(2018), pp. 956-964. ( RAAD 2017 Torino (Italia) 21-23 giugno 2017) [10.1007/978-3-319-61276-8\_102].

*Availability:*

This version is available at: 11583/2679186 since: 2023-10-13T10:21:17Z

*Publisher:*

Springer International Publishing

*Published*

DOI:10.1007/978-3-319-61276-8\_102

*Terms of use:*

This article is made available under terms and conditions as specified in the corresponding bibliographic description in the repository

*Publisher copyright*

(Article begins on next page)

# Control of force impulse in human-machine impact

**Carlo De Benedictis\*, Walter Franco, Daniela Maffiodo, Carlo Ferraresi**

Department of Mechanical and Aerospace Engineering, Politecnico di Torino, Torino, Italy  
carlo.debenedictis@polito.it

**Abstract** The clinical study of postural control requires a disturbance to be imposed to the subject under evaluation. Among various kinds of disturbance, a mechanical stimulation, consisting in an impulsive force impressed to a certain point of the body, can be used. This paper describes the study of a device conceived to generate such a disturbance. The device is based on a commercial pneumatic actuator, equipped with appropriate force and motion feedback sensors, and properly controlled. The major item is to take into account the interaction between the device and the human, in order to individuate the optimal control technique to generate the desired force pattern. A mathematical model of the device and the human-machine interaction is presented and a sliding mode control technique is proposed. Finally, the results of simulations are reported and discussed.

**Keywords:** Human-machine mechanical interaction · Postural control · Force perturbation · Force impulse control · Sliding mode control · Pneumatic servo-actuator

## 1. Introduction

Human-machine interaction is often related to the study and definition of safe contacts: many studies concern the evaluation of the effect of such contacts on the human body [11,16], while other work deals with the identification of safety requirements [10,13]; the problem of safe interactions is also related to the control of the robot itself [12,24].

The study of human-machine interaction has a significant impact in the design and optimization of collaborative robots (cobots) supporting human operators (i.e. in productive tasks [3] or to enhance the operator's skills [8]). Using a cobot as an assistive machine, i.e. to lift heavy loads, also can take advantage from the implementation of haptic systems [15].

Clinical applications of robotics often include a strict relationship between the device and several human operators; robots for aided surgery [9], for example, are relevant and complex technological systems, as well as robotic devices used to assist the patient during rehabilitation [20,23].

Due to the complexity of human-machine interaction, the choice of the control logic is relevant. In literature, hybrid force/position control is often discussed in this context [4], and the dynamic relation between position and force, specific of the system, is often managed by impedance control [14]: the impedance of the whole machine is continuously monitored and changed to exhibit specific mechanical characteristics towards the environment [21]. Some authors have proposed hybrid impedance [2] or force-impedance [1] control schemes, to overcome the limitations of the classical impedance control strategies. Due to the strongly nonlinear effects of friction, the control logics cited so far have relevant application in the control of pneumatically actuated systems [18].

Our work is oriented to the experimental study of human postural control. In these applications, a defined perturbation is often required to be exerted to the subject under evaluation; a possible form of perturbation could be to impart an impulsive force to the subject's body, to produce a variation of the body momentum. The aim of this work is to study a possible way of realizing a mechatronic device able to impress an impulse-controlled impact force on a surface.

This kind of application could require special solutions, as regards novel actuators [5], or original system architectures [17]. In our project, we adopted a pneumatic commercial cylinder, focusing in particular to the control logic. The work has been conducted on a model level, as a preliminary study, to verify the effectiveness of the pneumatic solution in this specific context.

## 2. The mathematical model

The system is described by the scheme of Fig.1 and is composed by a pneumatic double acting cylinder, two three-way flow-proportional valves and the impacted body. The latter is modeled as a mass able to translate along the direction of the hit, constrained to the frame by spring damper parallel network representing a purely passive human reaction to the impulsive disturbance. An additional damper-spring parallel network, interacting with the piston as an energy-absorbing buffer (Kelvin-Voigt material), simulates the human tissues. The mathematical model of the system runs on MATLAB-Simulink® environment. The parameters are collected in Table 1. The cylinder is described analytically by two continuity Equations (1), (2) and the dynamic equilibrium of the piston (3):

$$\dot{P}_a = \frac{G_a n R T_{ai}}{A_a (x_0 + x_{ma} + x) (P_a / P_{ai})^{(1-n)/n}} - \frac{P_a n}{(x_0 + x_{ma} + x)} \dot{x} \quad (1)$$

$$\dot{P}_b = \frac{G_b n R T_{bi}}{A_b (x_0 + x_{mb} - x) (P_b / P_{bi})^{(1-n)/n}} + \frac{P_b n}{(x_0 + x_{mb} - x)} \dot{x} \quad (2)$$

$$m\ddot{x} - (P_a - P_{ref})A_a + (P_b - P_{ref})A_b + F_e + F_{fr} = 0 \quad (3)$$

3

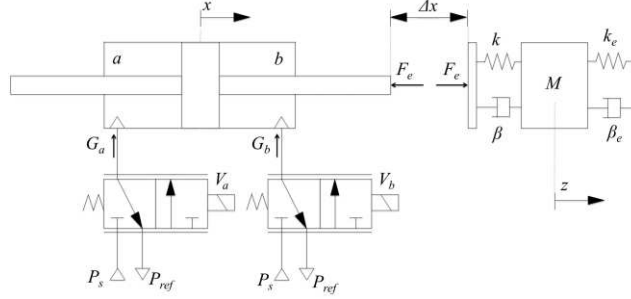


**Fig. 1.** Model of the system.

where  $x$  is the rod position,  $P$  is the absolute pressure in each chamber,  $P_i$  is the absolute initial pressure,  $P_{ref}$  is the absolute ambient pressure,  $G$  is the mass flow rate of air,  $T_i$  is the initial chamber temperature,  $n$  is the air polytropic coefficient,  $R$  is the air constant,  $A$  is the piston thrust section,  $x_0$  is half stroke of the cylinder,  $x_m$  is the chamber dead band of the piston,  $m$  is the mass of the moving parts,  $F_e$  is the resultant of the external forces exerted on the piston rod and  $F_{fr}$  is the piston force friction.

**Table 1.** Default parameters of the physical model.

Description	Symbol	Value
Rod diameter	$d_r$	10 mm
Cylinder diameter	$d_C$	50 mm
Piston translating mass	$m$	2 kg
Piston half stroke	$x_0$	50 mm
Chamber dead band	$x_m$	8 mm
Initial pressure in each chamber	$P_i$	1 bar
Initial temperature in each chamber	$T_i$	293 K
Air polytropic coefficient	$n$	1.4
Supply pressure	$P_s$	8 bar
Static friction force	$F_{st}$	20 N
Kinetic friction force	$F_{kin}$	15 N
Maximum valve conductance	$C_{max}$	$1.8 \cdot 10^{-8} \text{ Nm}^3/\text{s}/\text{Pa}$
Maximum voltage command (valve)	$V_{max}$	10 V
Valve time constant	$\tau_v$	5 ms
Body equivalent mass	$M$	70 kg
Body spring constant	$k_e$	3 kN/m
Body damper constant	$\beta_e$	1 kNs/m
Buffer spring constant	$k$	2 kN/m
Buffer damper constant	$\beta$	20 Ns/m
Impact stroke	$\Delta x$	10 mm

4

Each valve is modeled as a pneumatic resistance with variable section; their characteristics refer to the ISO 6358: considering  $P_u$  as upstream and  $P_d$  as downstream absolute pressures, the mass air flow is calculated in sonic or subsonic condition respectively (Eq. 4):

$$G = \rho_0 P_u C \text{ for } 0 < \frac{P_d}{P_u} \leq b, \quad G = \rho_0 P_u C \sqrt{1 - \left( \frac{P_d / P_u - b}{1 - b} \right)^2} \text{ for } b < \frac{P_d}{P_u} \leq 1 \quad (4)$$

where  $\rho_0$  is the air density in normal conditions,  $C$  is the conductance of the resistance and  $b$  is the critical ratio. Each valve is controlled by a bipolar voltage signal, whose relationship with the effective sectional area of the orifice is nonlinear. To consider the real characteristic of the system, the actual dead zone band in the relationship between conductance and voltage has been implemented, and a first order dynamic has been introduced considering the response time of the valve.

Since friction has a significant influence on the effectiveness of the control, the static-kinetic Coulomb friction model has been included, considering a force  $F_f$  acting on the piston, whose direction and value depend on the body motion.

The impact force,  $F_e$ , must be controlled to impart a specific impulse, affecting the momentum of the stricken body. The dynamic analysis of the body during the impact (i.e.  $F_e > 0$ ) yields the following equation:

$$F_e = k\varepsilon + \beta\dot{\varepsilon} = M\ddot{z} + \beta_e\dot{z} + k_e z, \quad \varepsilon = (x - \Delta x) - z \quad (5)$$

where  $z$  is the position of the body mass  $M$ ,  $k_e$  and  $\beta_e$  are respectively the coefficients of spring and damper constraining the body motion,  $\varepsilon$  is the actual deformation of the buffer representing the viscoelastic behavior of the human tissues,  $k$  and  $\beta$  are spring and damper coefficients of the buffer and  $\Delta x$  is the initial distance between the tip of the rod and the body (impact stroke). During the impact, the deformation  $\varepsilon$  is non-negative, as the contact force  $F_e$ .

### 3. Control logic

During the impact, the force  $F_e$  should be controlled to track a desired profile, in order to determine a variation in momentum of the stricken body  $M$  and to affect its dynamic response. Of course, before and after the impact, i.e. in the approach phase and in the actuator return to initial condition, the piston motion rather than the impact force must be controlled. To distinguish among the three phases of the device's action (approach, collision and return), an appropriate if-conditional block must be set. The control of the pneumatic cylinder can be defined in terms of the rod displacement or the impact force, depending on the operating phase.

5

In certain applications where human-machine interaction must be controlled, pure linear control logic can provide effective results [7]; in our case, the presence of nonlinear phenomena and the impulsive nature of the controlled force called for more sophisticated algorithms. Nonlinear control logics, currently used for the robust control of complex systems, have then been considered. In this work, the sliding mode control (SMC) technique has been chosen.

In the literature, several examples of this control technique are described, often applied to pneumatic actuators [25]. Sliding mode controllers are based on the definition of a sliding surface variable  $s$ , as an appropriate function of the error  $e$ . The problem of tracking ( $e=0$ ) is accomplished remaining on the surface for the time  $t>0$ , so controlling  $s=0$  (sliding mode condition). As proposed in literature [22], the sliding surface can be also defined by using integral control, considering the integral of the error as the variable of interest:

$$s = \left( \frac{d}{dt} + \lambda \right)^q \int_0^t e(r) dr \quad (6)$$

where the parameter  $\lambda$  can be selected arbitrarily, related to the dynamics of the error, while  $q$  is the order of the relationship between the variable to control and the control input. This formulation has been chosen for the cylinder position control during approach. Considering the voltage signal  $V$  generated by the control system as proportional to the valves' conductance  $C$ , the differentiation of Eq. 3 is required for the control input to appear. This leads to  $q=3$  and therefore:

$$s_x = \lambda_x^3 \int e_x + 3\lambda_x^2 e_x + 3\lambda_x \dot{e}_x + \ddot{e}_x, \quad e_x = x - x_{ref} \quad (7)$$

The force control, also implemented through SMC, uses a simpler formulation of the sliding surface as a function of the contact force error  $e_f$  [19]:

$$s_f = \dot{e}_f + \lambda_f e_f, \quad e_f = F_e - F_{ref} \quad (8)$$

The control input must be discontinuous across the sliding surface, to avoid the effect of disturbances and inaccurate modeling of the system. A standard (first order) SMC has been chosen, with the following control input, approximating a *sign* function [22]:

$$u = V = -K \operatorname{sat}\left(\frac{s}{\delta}\right), \quad \operatorname{sat}\left(\frac{s}{\delta}\right) = \begin{cases} s/\delta, & 0 \leq |s| < \delta \\ \operatorname{sign}(s), & |s| \geq \delta \end{cases} \quad (9)$$

where  $K$  is a positive constant, which cannot exceed the maximum admissible voltage accepted by the valves. The tuning of the constant parameter  $\delta$  defines the slope

6

of the control input. Both parameters have been set separately for the force ( $K_f$ ,  $\delta_f$ ) and position ( $K_x$ ,  $\delta_x$ ) controls.

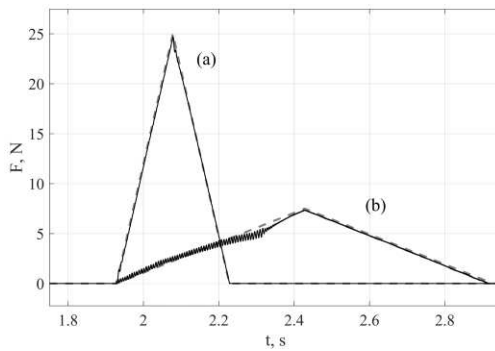
#### 4. Simulation and results

After tuning, the control parameters were set to the following values:  $\lambda_x=1$ ,  $\lambda_f=30$ ,  $K_x=K_f=10$ ,  $\delta_x=0.005$  and  $\delta_f=0.01$ .

The system has been simulated in two different conditions: initially, the stricken body has been represented by the unconstrained mass  $M$  free to translate along the direction of the collision, without considering the passive human reaction. This condition was adopted to verify the effectiveness of the force/position control of the pneumatic cylinder.

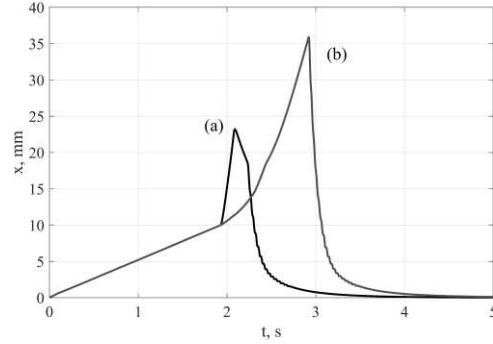
Figure 2 shows the tracking of two different force profiles having the same time integral, therefore producing the same variation of the body momentum. The control parameters tuning was based on the faster (a) profile, and also maintained for the other one (b). Although profile (b) shows a little *chattering* transient, the control has good tracking performance in both cases. Figure 3 shows the rod displacement corresponding to previous force profiles (a) and (b). The figure highlights the huge difference between the two operating conditions, in terms of piston displacement; nevertheless, the system shows dynamic performance able to guarantee the required task.

Figure 4 shows the control system response to the variation of the model parameters, as the buffer spring-damper coefficients ( $k$  and  $\beta$ ), to simulate different characteristic of tissues. The chosen values are coherent with data of literature [6]. The control system behavior appears to be significantly affected by these physical parameters, even if able to follow the desired force profiles for certain ranges. For example, a change of stiffness value  $k$  from 800 to 2000 N/m does not compromise the control performance. On the other hand, little changes in damping coefficient deeply influence the results.



**Fig. 2.** Tracking of two different force profiles sharing the same impulse (integral). The dashed line represents the reference force profile, while the solid one shows the actual contact force profile.

7



**Fig. 3.** Displacement of the piston rod in two different conditions of force tracking. The letters (a) and (b) refer to the corresponding force profile represented in Fig. 2.

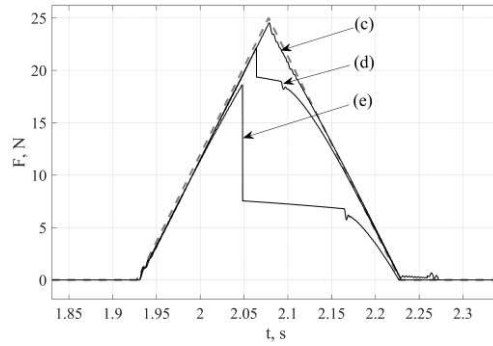


**Fig. 4.** Effects of model parameters on the control system. The dashed line represents the reference force profile, while the solid lines show the force tracking response for different choices of the tissues buffer coefficients:

- (c)  $k=800$  N/m,  $\beta=20$  Ns/m;
- (d)  $k=500$  N/m,  $\beta=8$  Ns/m;
- (e)  $k=200$  N/m,  $\beta=20$  Ns/m.

The condition of constrained mass has then been considered, checking the ability of the control to track the desired impulsive force profile and analyzing the effects on the stricken body, in terms of variation of momentum. Different values of the physical model parameters, related to the passive human reaction, namely the body spring  $k_e$  and damper coefficient  $\beta_e$ , have been set in order to verify the ability of the model to highlight a correlation between a given perturbation and the body response. Figure 5 shows the stricken body momentum  $Q$  versus time after the perturbation, when the same impulsive force is exerted. The different curves may describe the response of human subjects with different psycho-physical characteristics.

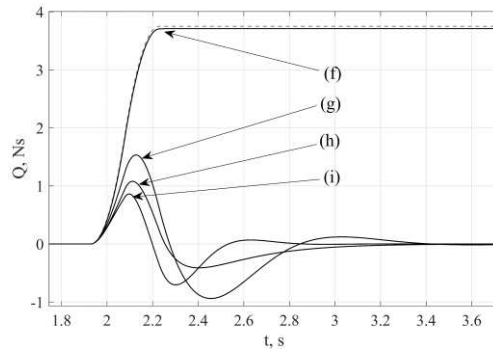


**Fig. 5.** Momentum variation of the stricken body. The dashed line is the impulse of the reference force profile; the solid lines show the momentum variation of the body, evaluated for different sets of the coefficients related to the human reaction:

- (f)  $k_e=0$  N/m,  $\beta_e=0$  Ns/m;
- (g)  $k_e=3000$  N/m,  $\beta_e=500$  Ns/m;
- (h)  $k_e=3000$  N/m,  $\beta_e=1000$  Ns/m;
- (i)  $k_e=10000$  N/m,  $\beta_e=1000$  Ns/m.



## 5. Conclusion

The results of the simulations showed the effectiveness of the SMC logic to use a pneumatic actuator for controlling an impulsive force to be exerted on a human. Different profiles of the contact force have been analyzed, as well as several combinations of the model parameters.

The simulations run with different profiles of the impulsive force showed the robustness of the adopted control logic.

On the other hand, the control system behavior emerged to be significantly affected by some physical parameters, namely the buffer spring and damper coefficients. Therefore, for a correct experimental use of the device, an accurate identification of such parameters will be important.

The simulations analyzing the momentum of the stricken body demonstrate that the device may be used to highlight some physiological characteristic of a human subjected to postural analysis.

## References

1. F. Almeida, A. Lopes and P. Abreu, "Force-Impedance Control: a new control strategy of robotic manipulators", Recent advances in Mechatronics, pp. 126–137, 1999.
2. R. J. Anderson and M. W. Spong, "Hybrid impedance control of robotic manipulators," IEEE Journal on Robotics and Automation, vol. 4, no. 5, pp. 549–556, 1988.
3. A. Cherubini, R. Passama, A. Crosnier, A. Lasnier and P. Fraisse, "Collaborative manufacturing with physical human–robot interaction", Robotics and Computer-Integrated Manufacturing, vol. 40, pp. 1-13, 2016.
4. S. Chiaverini and L. Sciavicco, "The parallel approach to force/position control of robotic manipulators," in IEEE Transactions on Robotics and Automation, vol. 9, no. 4, pp. 361-373, Aug 1993.
5. C. Ferraresi, W. Franco and G. Quaglia, "A novel bi-directional deformable fluid actuator", Proceedings of the Institution of Mechanical Engineers, Part C: Journal of Mechanical Engineering Science, vol. 228, no 15, pp. 2799-2809, 2014.
6. C. Ferraresi, D. Maffiodo and H.Hajimirzaalian, "A model-based method for the design of intermittent pneumatic compression systems acting on humans", Proc. IMechE Part.H: J. Eng. Med., vol. 228, no.2, pp. 118-126, 2014.
7. C. Ferraresi, D. Maffiodo and H.Hajimirzaalian, "Simulation and control of a robotic device for cardio-circulatory rehabilitation", Advances in Intelligent Systems and Computing, vol. 371, pp. 357-365, 2016.
8. C. Gosselin et al., "A Friendly Beast of Burden: A Human-Assistive Robot for Handling Large Payloads," in IEEE Robotics & Automation Magazine, vol. 20, no. 4, pp. 139-147, Dec. 2013.
9. S. Haddadin et al., "On making robots understand safety: Embedding injury knowledge into control", The International Journal of Robotics Research, vol. 31, no. 13, pp. 1578-1602, 2012.
10. S. Haddadin, A. Albu-Schäffer and G. Hirzinger, "Requirements for Safe Robots: Measurements, Analysis and New Insights", The International Journal of Robotics Research, vol. 28, no. 11-12, pp. 1507-1527, 2009.
11. S. Haddadin et al. "An Experimental Safety Study for Stab/puncture and Incised Wounds", IEEE ROBOTICS & AUTOMATION MAGAZINE, vol. 18, no. 4, pp. 20-34, 2011.

12. M. Heidingsfeld, R. Feuer, K. Karlovic, T. Maier and O. Sawodny, "A force-controlled human-assistive robot for laparoscopic surgery," 2014 IEEE International Conference on Systems, Man, and Cybernetics (SMC), San Diego, CA, 2014, pp. 3435-3439.
13. J. Heinzmann and A. Zelinsky, "Quantitative Safety Guarantees for Physical Human-Robot Interaction, The International Journal of Robotics Research, vol. 22, no. 7-8, pp. 479-504, 2003.
14. N. Hogan, "Impedance Control: An Approach to Manipulation: Part I—Theory", J. Dyn. Sys., Meas., Control, vol. 107, no.1, pp-1-7, 1985.
15. O. Khatib et al., "Human-Centered Robotics and Interactive Haptic Simulation", The International Journal of Robotics Research, vol. 23, no. 2, pp. 167-178, 2004.
16. B. Povse, S. Haddadin, R. Belder, D. Koritnik, and T. Bajd, "A tool for the evaluation of human lower arm injury: approach, experimental validation and application to safe robotics", Robotica, vol. 34, no. 11, pp. 2499–2515, Apr. 2015.
17. G. Quaglia, M. Scopesi and W. Franco, "A comparison between two pneumatic suspension architectures", Vehicle System Dynamics, vol. 50, no 4, pp. 509-526, 2012.
18. R. Richardson, M. Brown, B. Bhakta and M. Levesley, "Impedance control for a pneumatic robot-based around pole-placement, joint space controllers", Control Engineering Practice, vol. 13, no. 3, pp. 291-303, 2005.
19. E. Richer and Y. Hurmuzlu, "A High Performance Pneumatic Force Actuator System: Part II—Nonlinear Controller Design," Journal of Dynamic Systems, Measurement, and Control, vol. 122, no. 3, p. 426, 2000.
20. Y. Runze, L. Ji, and H. Chen, "Novel Human-Centered Rehabilitation Robot with Biofeedback for Training and Assessment," Universal Access in Human-Computer Interaction. Applications and Services, pp. 472–478, 2011.
21. M. Sharifi, S. Behzadipour, and G. Vossoughi, "Nonlinear model reference adaptive impedance control for human-robot interactions," Control Engineering Practice, vol. 32, pp. 9–27, Nov. 2014.
22. J. E. Slotine and W. Li, "Applied Nonlinear Control", Prentice Hall, 1991.
23. N. L. Tagliamonte et al., "Effects of Impedance Reduction of a Robot for Wrist Rehabilitation on Human Motor Strategies in Healthy Subjects during Pointing Tasks", Advanced Robotics, vol. 24, no. 5, pp. 537-562, 2012.
24. Y. Yamada, Y. Hirasawa, S. Huang, Y. Umetani and K. Suita, "Human-robot contact in the safeguarding space," in IEEE/ASME Transactions on Mechatronics, vol. 2, no. 4, pp. 230-236, Dec 1997.
25. Y. Zhu and E. J. Barth, "Impedance Control of a Pneumatic Actuator for Contact Tasks," Proceedings of the 2005 IEEE International Conference on Robotics and Automation, 2005, pp. 987-992.